PROGRESS IN THE PEELING-BALLOONING MODEL OF ELMS: TOROIDAL ROTATION AND 3D NONLINEAR DYNAMICS

by
P.B. SNYDER, H.R. WILSON, X.Q. Xu, and A.J. WEBSTER

JUNE 2004

DISCLAIMER

PROGRESS IN THE PEELING-BALLOONING MODEL OF ELMS: TOROIDAL ROTATION AND 3D NONLINEAR DYNAMICS

by
P.B. SNYDER, H.R. WILSON,* X.Q. Xu,[†] and A.J. WEBSTER*

This is a preprint of a paper to be presented at the 31st European Conf. on Plasma Physics and Controlled Fusion, London, United Kingdom, June 28 through July 2, 2004 and to be published in the *Proceedings.*

*EURATOM/UKAEA Culham Science Centre, Abingdon, United Kingdom.
[†]Lawrence Livermore National Laboratory, Livermore, California.

Progress in the Peeling-Ballooning Model of ELMs: Toroidal Rotation and 3D Nonlinear Dynamics

P.B. Snyder[1], H.R. Wilson[2], X.Q. Xu[3], and A.J. Webster[2]

[1]*General Atomics, P.O. Box 85608, San Diego, CA 92186-5608, USA*
[2]*EURATOM/UKAEA Culham Science Centre, Abingdon, Oxon OX13 3DB, UK*
[3]*Lawrence Livermore National Laboratory, Livermore, CA, USA*

Understanding the physics of the H-Mode pedestal and edge localized modes (ELMs) is very important to next-step fusion devices for two primary reasons: 1) The pressure at the top of the edge barrier ("pedestal height") strongly impacts global confinement and fusion performance, and 2) large ELMs lead to localized transient heat loads on material surfaces that may constrain component lifetimes. The development of the peeling-ballooning model has shed light on these issues by positing a mechanism for ELM onset and constraints on the pedestal height. The mechanism involves instability of ideal coupled "peeling-ballooning" modes driven by the sharp pressure gradient and consequent large bootstrap current in the H-mode edge. It was first investigated in the local, high-n limit [1], and later quantified for non-local, finite-n modes in general toroidal geometry [2,3]. Important aspects are that a range of wavelengths may potentially be unstable, with intermediate $n's$ ($n \sim 3\text{-}30$) generally limiting in high performance regimes, and that stability bounds are strongly sensitive to shape [Fig 1(a)], and to collisionality (i.e. temperature and density) [4] through the bootstrap current. The development of efficient MHD stability codes such as ELITE [3,2] and MISHKA [5] has allowed detailed quantification of peeling-ballooning stability bounds (e.g. [6]) and extensive and largely successful comparisons with observation (e.g. [2,6-9]). These previous calculations are ideal, static, and linear. Here we extend this work to incorporate the impact of sheared toroidal rotation, and the non-ideal, nonlinear dynamics which must be studied to quantify ELM size and heat deposition on material surfaces.
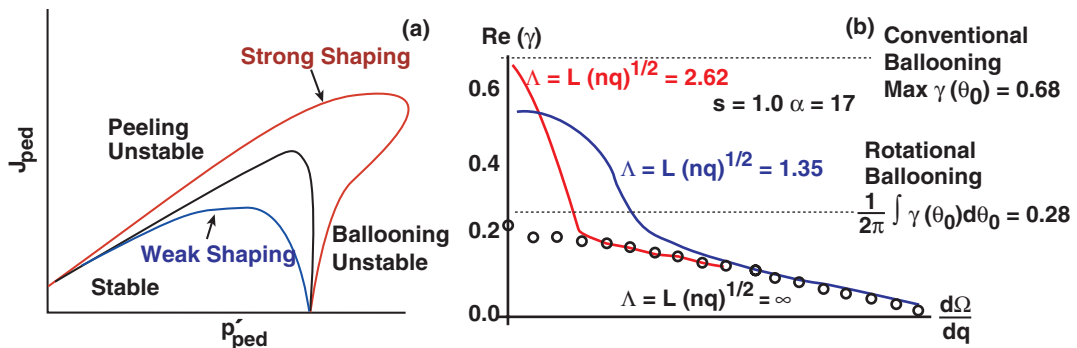

Fig. 1. (a) Schematic diagram of peeling-ballooning stability bounds vs. edge current and pressure gradient for different shaped equilibria. (b) Growth rate vs flow shear for n→∞ (circles) and for two finite values of *n*.

The effect of sheared toroidal rotation on ideal magnetohydrodynamic (MHD) instabilities has been previously studied for low n instabilities with numerical codes such as MARS (e.g. [10]), and also in the $n \to \infty$ limit, using eikonal methods [11,12]. For low n ideal modes in tokamaks, the effect of experimentally observed rotation is usually small. However, in the high n limit, the effect of rotation can be strongly stabilizing [11,12]. Specifically, in the $n \to \infty$, weak flow shear limit, flow shear leads to a reduction from the conventional static ballooning growth rate $\gamma(\theta_0)$, where θ_0 is chosen to maximize γ, to a rotationally averaged $\gamma = 1/2\pi \int \gamma(\theta_0) \, d\theta_0$ [11], resulting in a discontinuity in the predicted growth rate for very small flow. We have developed an eigenmode formalism, allowing finite-n and non-local geometry, in order to resolve this discontinuity and to allow calculation of flow shear effects on finite-n ballooning and peeling modes, including growth rate and mode structure. The formalism extends that given in Ref. [3] to include leading order flow shear ($n\Omega \sim 1$, $\Omega' \sim 1$) and compression terms. Initial studies employed this formalism in an s-α code, to connect with previous results and characterize important physics trends [13]. In the $n \to \infty$ limit [given by circles in Fig. 1(b)], the new formalism successfully reproduces the previous results given by Miller [12] using an eikonal method. The eigenmode formalism also resolves the low rotation discontinuity — in the s-α case this is done by incorporating an α profile, $\alpha = \alpha_0 \exp[-(1-r/r_0)^2/2L^2]$, where $\Lambda \equiv L(nq)^{1/2}$ characterizes the toroidal mode number n [13]. For large n [e.g. the $\Lambda=2.62$ case in Fig. 1(b)], a rapid transition from the conventional ballooning result (0.62) to the rotational ballooning occurs, while at lower n [e.g. $\Lambda=1.35$ in Fig. 1(b)], the transition is slower.

An important question then, is whether rotation shear strongly affects typical intermediate-n peeling-ballooning modes in observed conditions. To address this, we have incorporated the rotational formalism into the full ELITE code, and studied a number of cases. The result is that, as in the s-α case, there is a strong radial narrowing of the mode which occurs with increasing rotation shear. Very close to marginal stability ($\gamma/\omega_A \sim 10^{-3}$), substantial stabilization is possible. However, away from the marginal point, rotational shear generally has only a small effect on peeling-ballooning growth rates, and thus flow shear is not expected to measurably change the expected threshold for edge peeling-ballooning modes {a result consistent with the generally good agreement found in comparisons of static peeling-ballooning calculations with experiment (as in Refs. [2,6-9])}, though it may be more important in certain special cases such as low magnetic shear, and low aspect ratio. An example for DIII-D discharge 113207 is shown in Fig. 2. The most unstable mode (largest γ/ω_*) in the absence of rotation is $n=11$. Its growth rate (along with $n=8$) is shown in Fig. 2(a). While a small decrease in the compressionless growth rate occurs as rotation is increased toward the measured value (4 kHz), the change is very small, and indeed destabilization is found at large

rotation, and in the presence of compression (Γ=5/3). The real frequency of the mode scales roughly linearly with increasing rotation, matching $n\Omega$ just outside the pedestal top, near the middle of the mode. The mode width decreases with rotation as can be seen from Figs. 2(b,c). Fast CER measurements have recently allowed study of observed rotation profiles leading up to, and during ELMs (e.g. [14]). In a calculation using measured DIII-D profiles from discharge 115556 just before the ELM occurs, we find that the calculated eigenfrequency of the most unstable mode (n=9) is consistent with the observed rotation during the ELM (before the edge rotation decays following the ELM) [Fig. 2(d)].
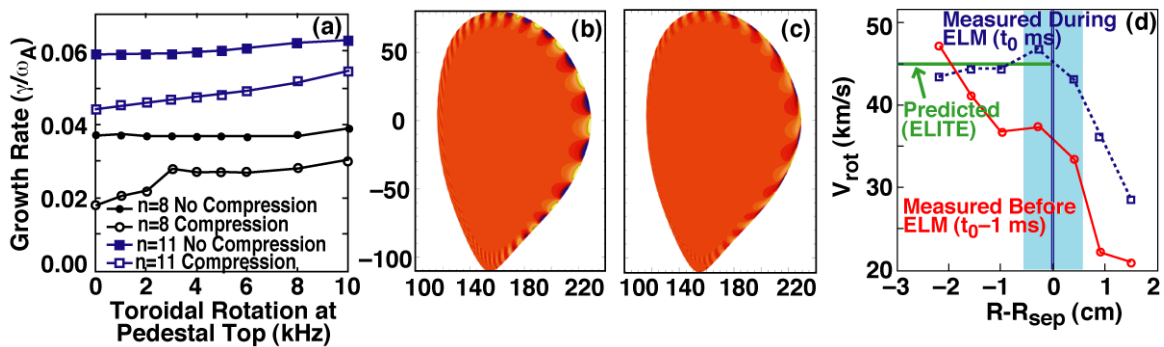

Fig. 2. (a) Growth rate vs. pedestal flow, and n=11 mode structure for (b) no flow and (c) Ω_{ped} = 10 kHz. (d) Measured rotation profile before and during an ELM. The measured rotation during an ELM is compared to the calculated mode rotation using pre-ELM profiles.

While linear stability studies have proved useful for understanding ELM onset and pedestal constraints, quantitative prediction of ELM size and heat deposition on material surfaces requires nonlinear dynamical studies. Nonlinear H-mode edge physics studies are in general quite challenging, due to the very wide range of relevant spatiotemporal scales, and the breakdown of a number of approximations (e.g. small perturbations, locality) that have simplified core simulations. Here we focus on the scales of the fast ELM crash event itself, initializing simulations with peeling-ballooning unstable equilibria and following the mode dynamics. We employ the 3D reduced Braginskii BOUT code [15], which uses field line following coordinates for efficiency, and simulates the pedestal and scrape-off layer (SOL) regions (typically $0.9 < \Psi < 1.1$). We study a DIII-D high density Type I ELMing equilibrium. In the early phases of the simulation, a fast growing mode is seen in the sharp gradient region of the pedestal, with approximately the growth rate and spatial structure expected from linear peeling ballooning calculations [Fig. 3(a), note that Δn=5 is used, hence what looks like n=4 in the 1/5 toroidal domain is an n=20 mode]. At later times (t > ~2000) a very fast burst occurs resulting in the rapid expulsion of particles across the separatrix, in a filamentary structure that is radially extended, but localized in the cross field (toroidal) direction

as shown in Fig. 3(b). Figure 3(c) shows the extended structure of the burst along the magnetic field, at a radial location just outside the separatrix. The filamentary burst has a number of characteristics that resemble ELM observations on DIII-D and MAST, and nonlinear ballooning theory predictions [16]. The fast growing, nonlinear bursting mode also appears consistent with the basic peeling-ballooning model, as the mode does not occur when parameters are lowered significantly below the linear peeling-ballooning threshold. Ongoing studies are focused on extending the duration of the nonlinear simulations, as well as extending their spatial extent, and eventually starting with a stable equilibrium and pushing it slowly across the peeling-ballooning stability threshold.
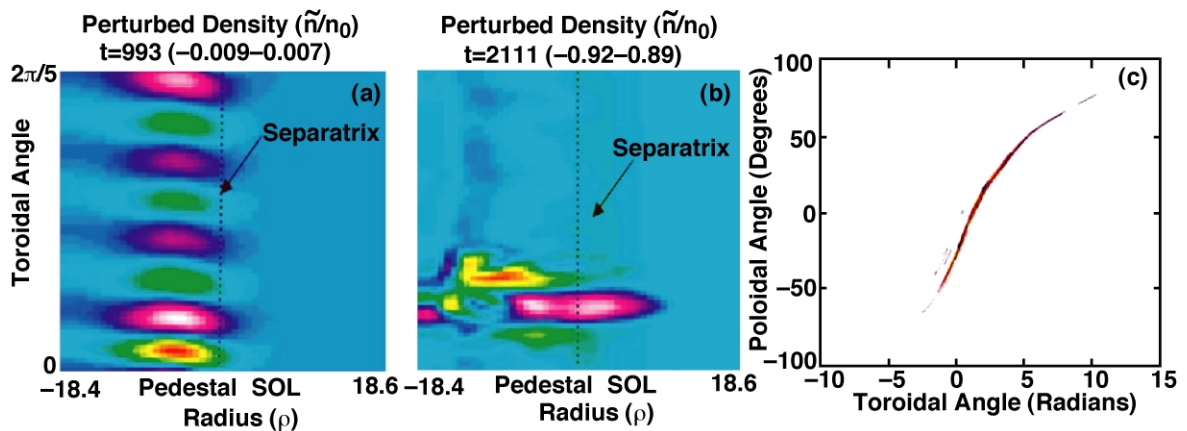

Fig. 3 (a) Density perturbation from nonlinear simulations at early times shows the expected peeling-ballooning structure (here *n*=20) in the pedestal region. (b) Later a fast radial burst across the separatrix occurs, localized toroidally, but extended along the field as shown in (c).

[1]   J.W. Connor, *et al.,* Phys. Plasmas **5** (1998) 2687; C.C. Hegna, *et al.,* Phys. Plasmas **3** (1996) 584.
[2]   P.B. Snyder, J.R. Wilson, J.R. Ferron, *et al.,* Phys. Plasmas **9** (2002) 2037.
[3]   H.R. Wilson, P.B. Snyder, *et al.,* Phys. Plasmas **9** (2002) 1277.
[4]   P.B. Snyder and H.R. Wilson, Plasma Phys. Control. Fusion **45** (2003) 1671.
[5]   G.T.A. Huysmans, *et al.,* Phys. Plasmas **8** (2002) 4292.
[6]   P.B. Snyder, H.R. Wilson, *et al.,* Nucl. Fusion **44** (2004) 320.
[7]   D.A. Mossessian, P.B. Snyder, A. Hubbard, *et al.,* Phys. Plasmas **10** (2003) 1720.
[8]   S. Saarelma, *et al.,* Nucl. Fusion **43** (2003) 262.
[9]   L.L. Lao, Y. Kamada, T. Okawa, *et al.,* Nucl. Fusion **41** (2001) 295.
[10]   M.S. Chu, *et al..* Phys. Plasmas **2** (1995) 2236.
[11]   F.L. Waelbroeck and L. Chen, Phys Fluids **B3** (1991) 601.
[12]   R.L. Miller, F.L. Waelbroeck, A.B. Hassam and R.E. Waltz, Phys. Plasmas **2** (1995) 3676.
[13]   A.J. Webster and H.R. Wilson, Phys. Rev. Lett. **92** (2004) 165004; A.J. Webster and H.R. Wilson, Phys. Plasmas **11** (2004) 2135.
[14]   J.A. Boedo, *et al.,* submitted to Phys. Rev. Lett. (2004)
[15]   X.Q. Xu, *et al.,* New J. Physics **4** (2002) 53.
[16]   H.R. Wilson and S.C. Cowley, Phys. Rev. Lett. **92** (2004) 175006.